

Supplementary Information

Alkaline Electro-activated Fe-Ni Phosphide Nanoparticle-Stack Array for High-performance Oxygen Evolution under Alkaline and Neutral Conditions

*Bowei Zhang, Yu Hui Lui, Lin Zhou, Xiaohui Tang, and Shan Hu**

B. Zhang, Y. H. Lui, X. Tang, S. Hu
Department of Mechanical Engineering
Iowa State University
Ames, IA 50011, USA
E-mail: shanhu@iastate.edu

L. Zhou
Ames National Lab, US Department of Energy
Ames, IA 50011, USA

Experimental Section

Materials and chemicals: Nickel foam (thickness, 1.6 mm; bulk density, 0.45 g/cm³) was purchased from Sigma Aldrich. NH₄F, urea, RuO₂ powder, and NaH₂PO₂·H₂O were provided by Sigma Aldrich. Ni(NO₃)₂·6H₂O and Fe(NO₃)₃·9H₂O were purchased from Fisher Scientific. All chemicals used in this work are of analytical grade. The deionized (DI) water used through this work was purified by Milli-Q system.

Synthesis of FeNi-OH/NF and FeNi-P/NF: Nickel foams (NF, 2 cm × 3 cm) were carefully cleaned with the assistance of sonication to remove surface oxide in 6 M HCl, ethanol, and DI water for 15 min, respectively. To synthesis Fe-Ni hydroxide on nickel foam (FeNi-OH/NF), 4 mmol of NH₄F, 10 mmol urea, and 4 mmol total amount of Ni(NO₃)₂·6H₂O and Fe(NO₃)₃·9H₂O were dissolved in 40 mL Milli-Q-water with the Fe/Ni ratios of 10:0, 9:1, and 7:3; respectively. Then the solution and the cleaned nickel foam were transferred into a 50 mL Teflon-lined stainless steel autoclave, then sealed and kept at 120 °C for 6 h with a heating rate of 3 °C min⁻¹ for hydrothermal growth of the hydroxides on nickel foam, followed by washing the obtained samples with DI water under the assistance of sonication and dried at 60 °C for 6 h. To prepare the phosphide on nickel foam, the as-synthesized hydroxides and 1.6 g of NaH₂PO₂·H₂O were put at two separate positions in a ceramic boat inside a tube furnace with NaH₂PO₂·H₂O powder at the upstream of the gas flow. After flushed with argon (Ar) to wash the quartz tube for about 30 minutes, the center of the tube furnace was elevated to 300 °C at a ramping rate of 3 °C min⁻¹ and kept at this temperature for 2 hour in a static Ar atmosphere. After that, samples were cooled to ambient temperature in the atmosphere of Ar. The black nickel foam was the desired product and can be used as the electrode directly. When Fe/Ni ratio of the starting solution is 3/7, the corresponding products of hydroxide and phosphide are denoted as FeNi-OH/NF and FeNi-P/NF in this work, respectively.

Materials characterization: The crystallographic information was characterized by XRD (Siemens D500 X-ray diffractometer) using Cu K α radiation. The morphology and structure of the materials were characterized using a FEI Titan Themis 300 Cubed probe aberration corrected STEM and a FEI Quanta 250 field-emission scanning electron microscopy (FE-SEM). X-ray photoelectron spectroscopy (XPS, AMICUS ESCA 3400) measurements were performed with Mg K α 1253.7eV radiation. The Fe/Ni ratio of active material was determined by inductively coupled plasma emission spectrometer (ICP-MS).

Electrochemical activation: The above as-synthesized electrodes were directly used as working electrodes and the electrochemical activation processes were performed in 1M KOH solution using 20 cyclic voltammogram (CV) cycles with Pt wires as the counter electrode and Hg/HgO electrode as the reference electrode. Cyclic voltammograms were conducted from -0.4 to 0.6 V vs Hg/HgO at a scan rate of 100 mV/s. After the alkaline activation, the electrodes were denoted as FeNi-P/NF-A, FeNi-OH/NF-A, and Ni-P/NF-A, respectively. All of the activated samples were rinsed with DI water and dried in air at room temperature.

Electrochemical measurements: All electrochemical measurements were conducted on a Gamry Interface 3000 potentiostat at room temperature in a three-electrode setup using electrocatalysts electrode as the working electrode, a Pt wire as the counter electrode, and Ag/AgCl (3M) and

Hg/HgO electrodes as the reference electrodes. OER tests were performed in 0.1 M phosphate buffer solutions (pH=7.0) and 1 M KOH (pH=13.6), respectively, at room temperature. All potentials measured were calibrated to RHE using the following equations: $E(RHE) = E_{Hg/HgO} + 0.098 + 0.059pH = E(Ag/AgCl) + 0.197 + 0.059pH$. Polarization curves were obtained using linear sweep voltammetry (LSV) with a scan rate of 5 mV. It needs to be noted that all of the LSV curves were recorded after about 10 CV cycles in the corresponding media until the curves were stable and corrected by IR-compensation unless otherwise noted. The long-term stability tests were carried out using the chronopotentiometric measurements and CV. The loading mass of the phosphide on nickel foam is about 3.3 mg/cm². RuO₂ ink was prepared by dispersing 10 mg RuO₂ powder in the mixture solution of 950 μL ethanol and 50 μL Nafion (20 wt. %). Then the as-prepared ink was coated onto nickel foam with the loading mass density of about 3.5 mg/cm² and dried in air at 60 °C. Electrochemical impedance spectroscopy (EIS) measurements were carried out in a frequency range from 10⁵ Hz to 0.1 Hz.

Turnover frequency (TOF) calculation: The turnover frequency (TOF) value is calculated according to the equation: $TOF = (j \times A) / (4 \times F \times n)$. j is the current density. A is the geometric area of the electrode. F is the faraday constant (96485 C/mol). n is the number of moles of the active materials that are integrated on nickel foam. $n = m/M$, m is the mass of active material on nickel foam; M is the molecular weight of the corresponding active material. All the Ni atoms and Fe atoms were assumed to be accessible for the catalysis.

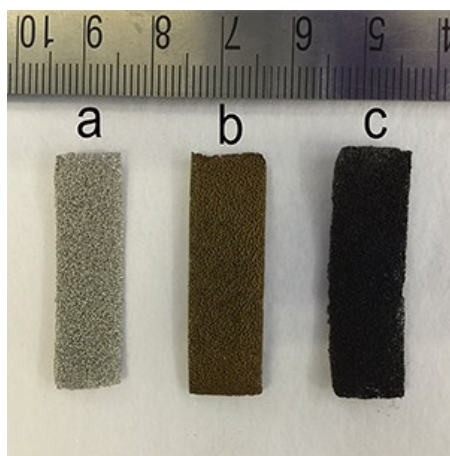


Figure S1. Photographs of (a) the nickel foam (NF), (b) FeNi-OH/NF, and (c) FeNi-P/NF.

The optimization process of the electrodes (Figure S2-S4)

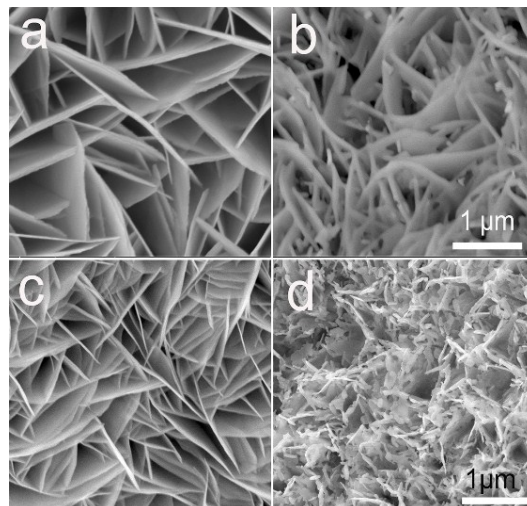


Figure S2. SEM images of (a) Ni hydroxide and (b) Ni phosphide on nickel foams. (c) (Fe_{0.1}Ni_{0.9})-hydroxide precursor and (d) its corresponding phosphide on nickel foams.

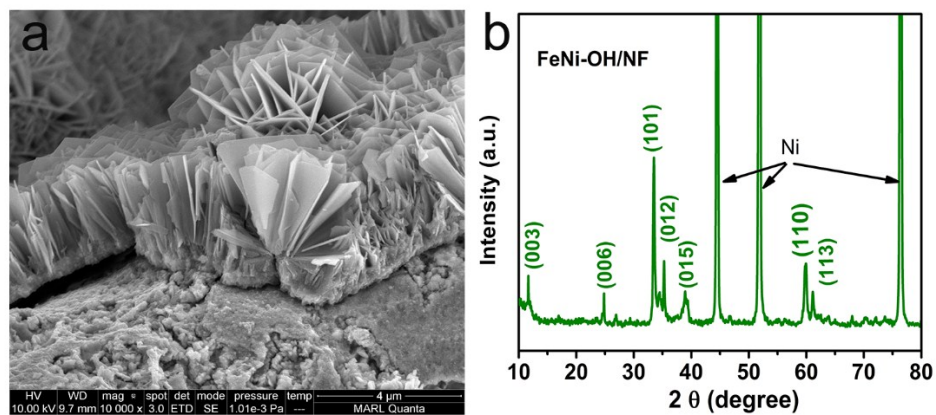


Figure S3. a) The side-view of the FeNi hydroxide nanosheet arrays on nickel foam and b) the corresponding XRD pattern.

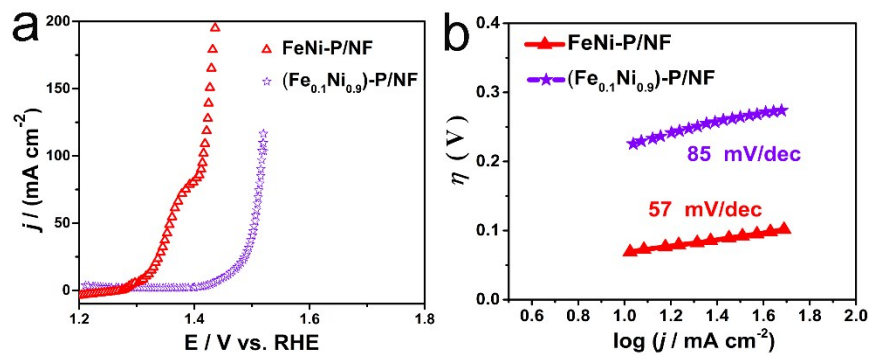


Figure S4. (a) OER polarization curves and (b) the corresponding Tafel slope for FeNi-P/NF and (Fe_{0.1}Ni_{0.9})-P/NF in 1M KOH solution.

Note: It is impossible to synthesize Fe hydroxide nanosheets on nickel foam,^[1,2] thus its corresponding phosphides cannot be obtained for a control.

1. **Nano Lett.**, 2016, 16, 6617.
2. **Nat. Commun.**, 2016, 7, 12324.

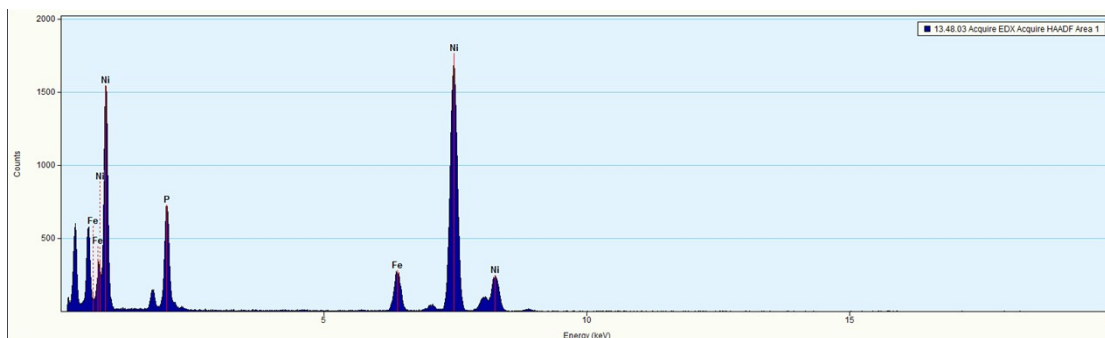


Figure S5. EDX spectrum of FeNi-P.

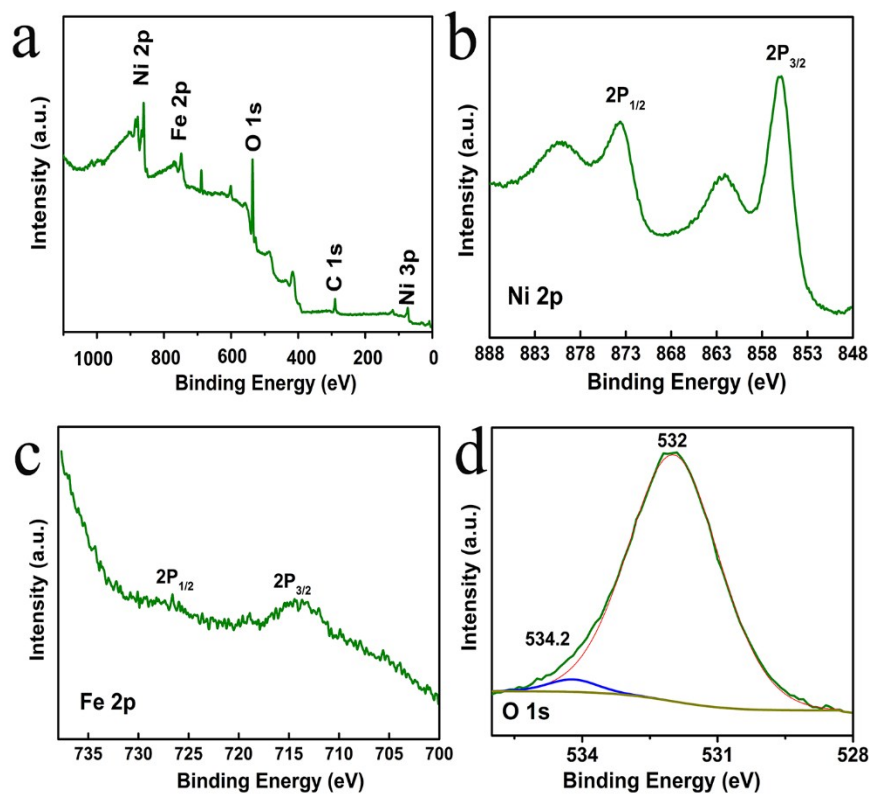


Figure S6. (a) XPS survey spectra of FeNi-OH. High resolution XPS spectrum of (b) Ni 2p, (c) Fe 2p, and (d) O1s in FeNi-OH.

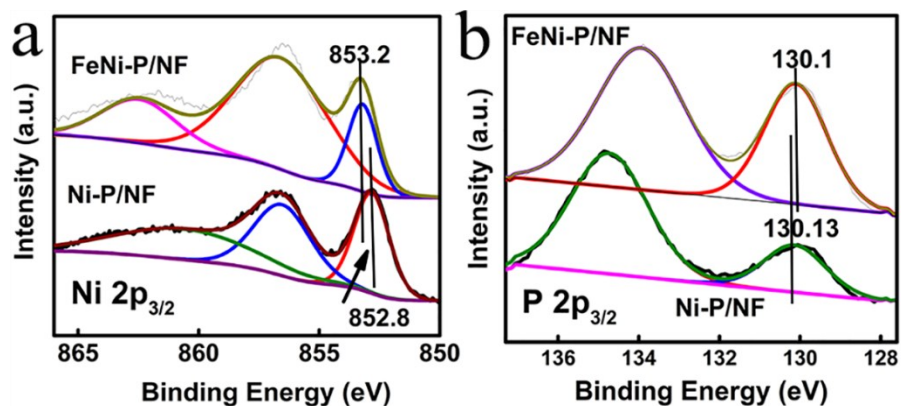


Figure S7. Detailed XPS spectra of (a) Ni 2p_{3/2} and P 2p_{3/2} for Fe-Ni phosphide (FeNi-P) and Ni₂P (Ni-P), respectively. Compared to Ni phosphide, the positive shift of Ni bonding energy and negative shift of P bonding energy can be observed after the Fe incorporation into Ni-P.

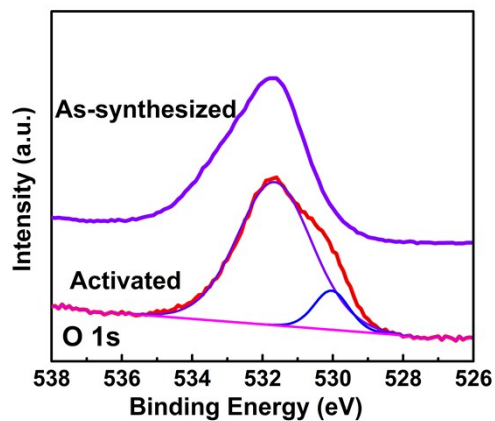


Figure S8. High-resolution XPS spectrum of O1s for FeNi-P and alkaline electro-activated FeNi-P (FeNi-P-A).

Electrochemical active surface area (ECSA)

The active surface area of each catalyst was measured from their electrochemical capacitances in a non-faradic region using a simple cyclic voltammetry method. The double layer current is equal to the product of the scan rate and the capacitance, which is expected to be linearly proportional to the active surface area of electrode. The current density differences were obtained at the potential of 0.92 V vs. RHE. By plotting the capacitive currents ($J_{\text{anodic}} - J_{\text{cathodic}}$) versus scan rate, the capacitance can be estimated as half of the slope.

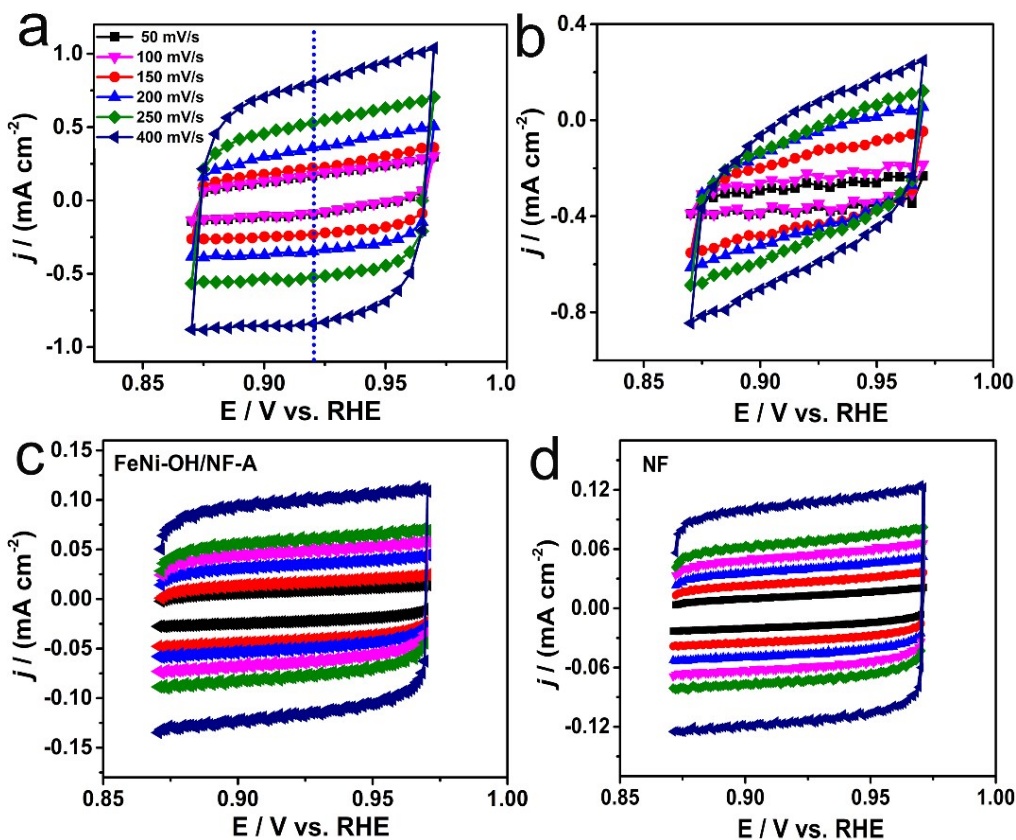


Figure S9. Electrochemical capacitance measurements of the relative ECSA of FeNi-P/NF-A and Ni-P/NF-A in 1M KOH. Cyclic voltammograms in the region of 0.87 to 0.97 V vs RHE of (a) FeNi-P/NF-A, (b) Ni-P/NF-A, (c) FeNi-OH/NF-A, and (d) the bare Ni

Methylene blue (MB) adsorption method

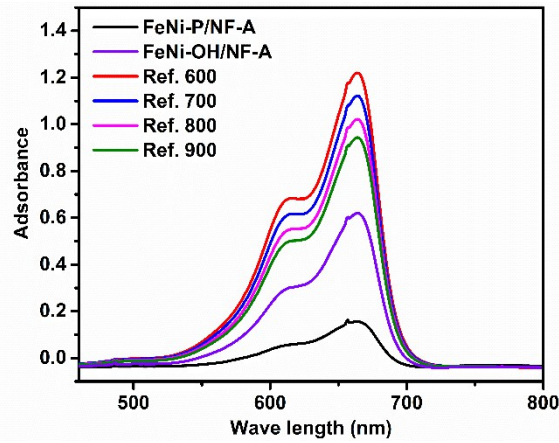


Figure S10. The MB absorbance spectrum for FeNi-P/NF-A, FeNi-OH/NF-A, and the standard reference MB solutions (diluted from 600 times to 900 times). According to the absorbance spectrum, the SSA of FeNi-P/NF-A is about 3.3 times of FeNi-OH/NF-A.

Methylene blue (MB) adsorption method was used to compare the specific surface area (SSA) of FeNi-P/NF-A and FeNi-OH/NF-A electrodes by UV-vis absorbance spectrum at 664nm. MB solution of known concentration $C_{MB}^0 = 2 \text{ mg mL}^{-1}$ is diluted at 600, 700, 800, and 900 times and the corresponding concentrations were plotted against the intensity of UV-vis light absorbance at 664nm for constructing a working curve. This working curve is then used to determine concentration of MB (C_{MB}) in the measured samples using UV-vis light absorbance of the sample.

FeNi-P/NF-A and FeNi-OH/NF-A electrodes with the same geometry area (A) are immersed into 10 mL of 2 mg mL^{-1} solution in two separate vials and keep for 24 hours to reach MB adsorption equilibrium. The resulting solutions are diluted for 1200 times for the measurement. The resulting solution concentration are calculated through the previous constructed reference working curve. The mass of the absorbed MB is calculated through:

$$m_{MB} = (2 \text{ ml} \times 2 \text{ mg mL}^{-1}) - C_{MB,i} \times (2.0 \text{ mL}), \quad i = \text{FeNi-P/NF-A or FeNi-OH/NF-A}$$

The SSA was calculated using following equation:

$$SSA(\text{m}^2 \text{ cm}^{-2}) = K \times \frac{m_{MB}}{A}$$

K is a constant that stands for the area (in m^2) covered by 1mg of MB and A (cm^2) is the geometric area of the sample.

Using the absorbance at 664nm shown in Figure S10, the estimated SSA of FeNi-P/NF-A is 3.3 times of FeNi-OH/NF-A, indicating the phosphorization treatment effectively tuned the morphology of FeNi hydroxide precursor and improved the SSA.

LSV curves normalized by electrochemical active surface area (ECSA):

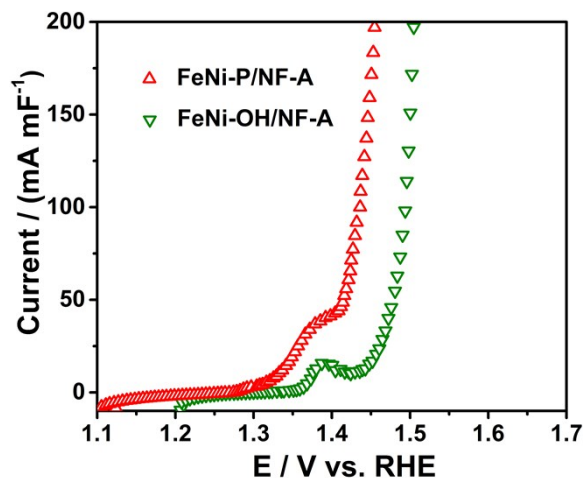


Figure S11. Polarization curves normalized by the ECSA.

Table S1 Mass loading of alkaline electrochemical activated Ni-P and FeNi-P on Ni foams.

Catalyst	mg/cm ²
Ni-P/NF-A	3.74 ± 0.42
FeNi-P/NF-A	2.86 ± 0.33

The mass loading of Fe-Ni phosphide slightly decreases after the Fe introduction, indicating its enhanced OER performance (as shown in Figure 3a and b) is aroused by Fe incorporation rather than the increase of catalyst mass loading density.

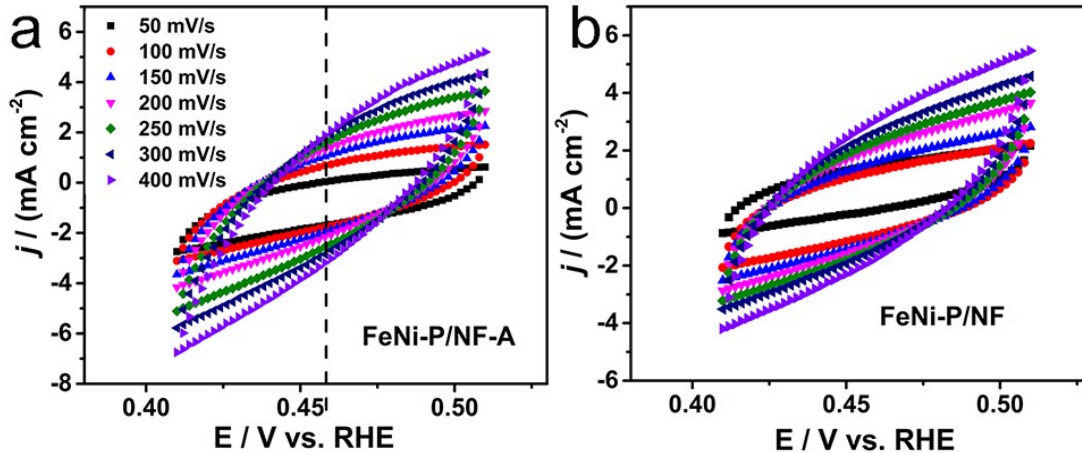


Figure S12. Electrochemical capacitance measurements of the relative ECSA of FeNi-P/NF-A and FeNi-P/NF electrodes upon OER in 0.1 M KPi. CV cycles were conducted in the region of 0.41 to 0.51 V vs RHE. The current density differences were obtained at the potential of 0.46 V vs RHE.

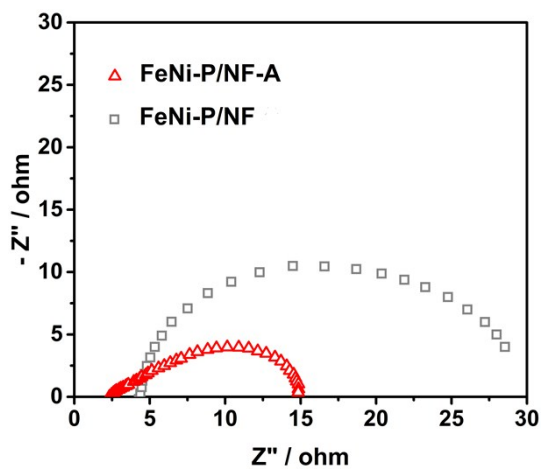


Figure S13. Nyquist plots of FeNi-P/NF-A and FeNi-P/NF. The frequency range of EIS is from 100 kHz to 0.1 Hz at a potential of 1.8 V vs RHE.

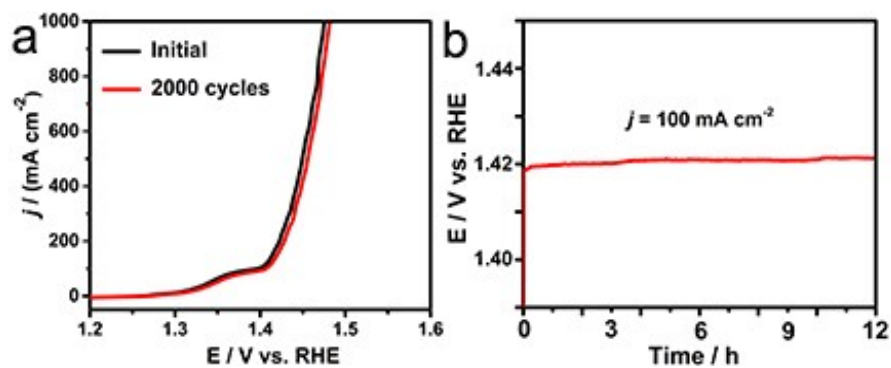


Figure S14. The stability tests for FeNi-P/NF-A electrode in 1M KOH media.

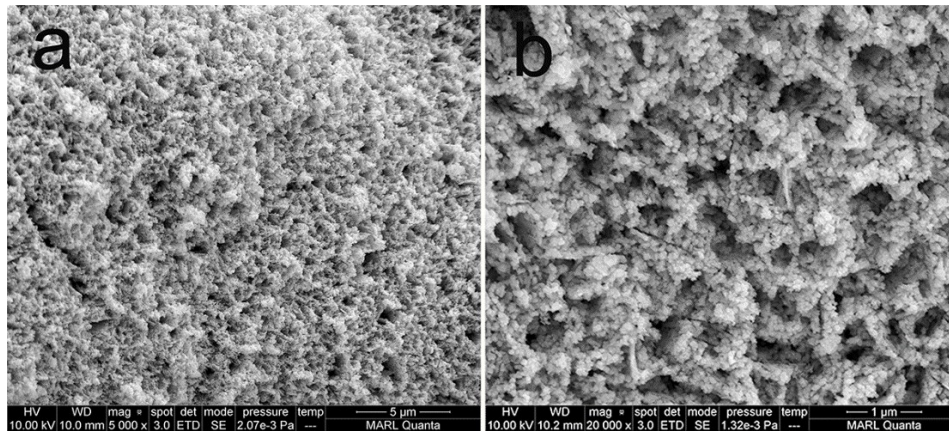


Figure S15. SEM image of FeNi-P/NF-A after the stability test in 1M KOH. The unique structure of interconnected FeNi phosphide nanoparticles still preserved well.

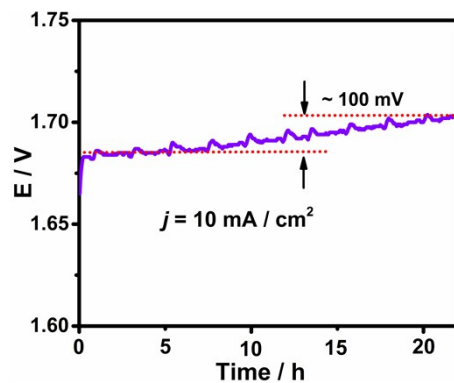


Figure S16. Stability test for FeNi-P/NF-A in 0.1 M KPi at 10 mA/cm². After 23 hours test, a slight colour change (from transparent to light yellow-green) of the electrolyte could be observed, indicating the dissolution of Fe/Ni into the electrolyte.

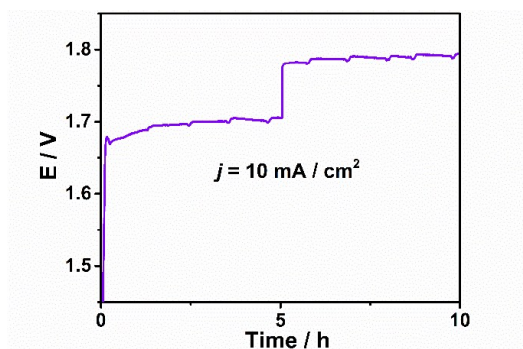


Figure S17. Long-term durability test of FeNi-P/NF-A with a lower mass loading (1.1 mg/cm²) in 0.1M KPi at 10 mA/cm². The hydroxide precursor of this electrode was obtained by reducing the hydrothermal time to 1h.

Table S2. Comparison of recently reported non-precious metal electrocatalysts for OER in alkaline medium. (j : current density; η : overpotential)

Catalyst	Medium	$j/\text{mA cm}^{-2}$	η/mV	Reference
FeNi-P/NF-A	1M KOH	100	186	<i>This work</i>
		500	235	
G-FeCoW/Gold foam	1M KOH	10	191	<i>Science</i> 2016 , 352, 333-337.
$\text{Ni}_x\text{Fe}_{1-x}\text{Se}_2\text{-DO/Ni}$ foam	1M KOH	10	195	<i>Nat. Commun.</i> 2016 , 7,12324.
NiFe hydroxide/Ni foam	1M KOH	10	215	<i>Nat. Commun.</i> 2015 , 6, 6616.
		80	270	
	10M KOH	500	240	
		1000	270	
$\text{Ni}_{60}\text{Fe}_{30}\text{Mn}_{10}$	1M KOH	500	360	<i>Energy Environ. Sci.</i> 2016 , 9, 540-549.
FeOOH/Co/FeOOH /Ni foam	1M NaOH	21	250	<i>Angew. Chem. Int. Ed.</i> 2016 , 55, 3694-3698.
		91	300	
		199	350	
CoFeNiO _x /Ni foam	1M KOH	10	240	<i>J. Am. Chem. Soc.</i> 2016 , 138, 8946-8957.
		100	272	
Ni:Pi-Fe/Ni foam	1M KOH	500	290	<i>Chem. Mater.</i> 2016 , 28, 5659-5666.
	5M KOH	1600	332	
Co/Co ₂ P/Ni foam	1M KOH	50	190	<i>ACS Energy Lett.</i> 2016 , 1, 1192-1198.
Fe-CoP/Carbon cloth	1M KOH	10	230	<i>Adv. Mater.</i> 2016 , DOI: 10.1002/adma.201602441.
MoS ₂ /Ni ₃ S ₂ /Ni foam	1M KOH	10	218	<i>Angew. Chem.</i> 2016 , 128, 6814-6819.
MoO ₂ /Ni foam	1M KOH	10	260	<i>Adv. Mater.</i> 2016 , 28, 3785-3790.
Ni _{0.51} Co _{0.49} P/Ni foam	1M KOH	10	239	<i>Adv. Funct. Mater.</i> 2016 , 26, 7644-7651.
FeNi ₃ N/Ni foam	1M KOH	10	202	<i>Chem. Mater.</i> 2016 , 28, 6934-6941.

Table S3. Comparison of the recently reported representative non-precious metal based electrocatalysts for OER in neutral medium. (j : current density; η : overpotential)

Catalyst	PBS	$j/\text{mA cm}^{-2}$	η/mV	Reference
FeNi-P/NF-A	0.1 M	10	429	<i>This work</i>
Co-Pi/Ti	0.1 M	10	450	<i>Angew. Chem.</i> 2017 , 129, 1084-1088.
	0.5 M	10	420	
	1.0 M	10	380	
Co-B _i NS/G	Not mentioned	14.4	570	<i>Angew. Chem. Int. Ed.</i> 2016 , 55, 2488-2492.
Co-TpBpy	0.1 M	1	400	<i>Chem. Mater.</i> 2016 , 28, 4375-4379.
Ni ₂ WO ₆ nanoplates	0.5 M Na ₂ SO ₄	10	540	<i>J. Mater. Chem. A</i> , 2016 , 4, 2438-2444
NGCO	0.1 M	1	410	<i>Nanoscale Horiz.</i> 2016 , 1, 41-44.
Co1/MWCNT rinsed	0.1 M	1	330	<i>ACS Catal.</i> , 2016 , 6, 6429-6437.
CoO/CoSe ₂	0.5 M	33.96	620	<i>Adv. Sci.</i> 2016 , 3, 1500426.
Co ₃ S ₄ Nanosheets	Not mentioned	3.97	700	<i>Angew. Chem. Int. Ed.</i> 2015 , 54, 11231.
Fe-based film	0.1 M	1	530	<i>Angew. Chem. Int. Ed.</i> 2015 , 54, 4870-4875.
Ni	0.5 M (pH=9.2)	1	540	<i>J. Am. Chem. Soc.</i> 2015 , 137, 13980.
Co ₃ O ₄ nanorod	0.1 M	1	385	<i>Electrocatal.</i> 2015 , 6, 331-340.
Mn ₅ O ₈	0.3 M	5	580	<i>ACS Catal.</i> 2015 , 5, 4624-4628.